Grain boundary self-diffusion in Ni: Effect of boundary inclination

Mikhail I. Mendelev,[a] Hao Zhang,[b] and David J. Srolovitz[c]
Department of Mechanical & Aerospace Engineering, Princeton University, Princeton, New Jersey 08540

(Received 20 October 2004; accepted 22 December 2004)

We examined the influence of the boundary plane on grain-boundary diffusion in Ni through a series of molecular dynamics simulations. A series of ⟨010⟩ Σ5 tilt boundaries, including several high symmetry and low symmetry boundary planes, were considered. The self-diffusion coefficient is a strong function of boundary inclination at low temperature but is almost independent of inclination at high temperature. At all temperatures, the self-diffusion coefficients are low when at least one of the two grains has a normal with low Miller indices. The grain boundary self-diffusion coefficient is an Arrhenius function of temperature. The logarithm of the pre-exponential factor in the Arrhenius expression was shown to be nearly proportional to the activation energy for diffusion. The activation energy for self-diffusion in a (103) symmetric tilt boundary is much higher than in boundaries with other inclinations. We discuss the origin of the boundary plane density–diffusion coefficient correlation.

I. INTRODUCTION

A complete crystallographic description of a flat grain boundary requires the specification of five independent variables: three associated with the misorientation of the two grains with respect to one another and two to describe the orientation of the boundary plane. Many grain boundary properties (e.g., grain boundary energy, self-diffusion coefficients, mobility, and electrical resistance) are sensitive to these five crystallographic parameters. Since preparation of well-controlled bicrystals is significantly more difficult than that for polycrystalline samples, most such properties are reported as polycrystalline averages. Further, many bicrystal studies (e.g., of grain boundary migration) are performed on curved boundaries, where only three of these five parameters are fixed.[1,2] An additional difficulty in describing the variation of grain boundary properties with these crystallographic and the remaining physical parameters (e.g., temperature) is associated with the large dimensionality of the parameter space. As a result, most systematic studies of boundary properties focus only on either misorientation or boundary plane. Of these, almost all have focused on the misorientation variables. In the present study, we fix the misorientation and examine the effect of varying the grain boundary plane on grain boundary self-diffusion in Ni.

Our focus on grain boundary diffusivity was motivated by the fact that the self-diffusion coefficient is sensitive to grain boundary structure. Many earlier studies have examined the relation between grain boundary thermodynamics and grain boundary structure.[3] Systematic studies of the dependence of grain boundary kinetic properties (e.g., grain boundary mobility) on grain boundary structure have been few. While several experiments have been performed to determine the grain boundary self-diffusion coefficient in Ni, the reported activation energies exhibit considerable variation.[4–9] This may, in part, be attributable to variations in the grain boundary character distribution with sample preparation technique and the natural variation of boundary inclination that occurs in polycrystalline samples. We addressed some of the issues by performing a series of molecular dynamics (MD) simulations of self-diffusion in a Σ5 36.8° ⟨001⟩ tilt boundary in nickel as a function of the inclination of the boundary plane and temperature. We then attempt to understand the effects of boundary inclination by seeking correlations between the diffusivity and both grain boundary structural features and grain boundary energy.

In the next section, we briefly describe the grain boundary bicrystallography, the simulation method, and

[a]Present address: Ames Laboratory, 207 Metals Development, Ames, Iowa, 50011
[b]Address all correspondence to this author.
e-mail: hzhang@princeton.edu
[c]This author was an editor of this journal during the review and decision stage. For the *JMR* policy on review and publication of manuscripts authored by editors, please refer to http://www.mrs.org/publications/jmr/policy.html.
DOI: 10.1557/JMR.2005.0177

the method used to determine grain boundary self-diffusivity. Then we present the grain boundary self-diffusivity data as a function of temperature to extract the activation energy and pre-exponential factor for ten different boundary inclinations. In the last section of this report, we correlate these data with boundary structure and energy to gain insight into the relationship between kinetic, structural, and thermodynamic properties of grain boundaries.

II. SIMULATION METHOD

The bicrystal is constructed in the following manner: (i) generate two identical, overlapping, face centered cubic lattices (A and B), (ii) rotate lattice B with respect to lattice A about a [010] axis by 36.87° (i.e, $\Sigma 5$), (iii) choose a (boundary) plane that includes the [010] direction and remove all atoms in the A lattice below the plane and remove all atoms in the B lattice above the plane, and (iv) if any two atoms are closer than 0.1 nm, remove one of them. The angle describing the orientation of the boundary plane is arbitrary. We set this angle α to zero for the highest atomic density boundary plane. This corresponds to a symmetric boundary with a (103) boundary plane, as seen in Fig. 1(a). For any value of α, we rotate the bicrystal such that the boundary lies in the *x-y* plane of the simulation cell. Examples of the initial simulation unit cell for three different boundary planes [values of α measured with respect to the (103) plane in the lower crystal] are shown in Fig. 1. Note, in all cases, the misorientation of the two grains with respect to each other is always 36.87°. The simulation cell has free top and bottom surfaces ($\pm z$) at least 5.0 nm above/below the boundary plane. The width of the simulation cell (*x* and *y* directions) is in the 5–7 nm range, depending on the periodicity of the bicrystal. We limit our choice of boundary inclinations to cases where the periodicity of the two grains is commensurate in the plane of the boundary. For instance, for $\alpha = 26.6°$, the boundary plane is corresponding to (107) and (101) surfaces in the upper and lower crystals, respectively. These surfaces have the same periodicity in the *y* direction and the repeat distance in the *x* direction of the upper crystal is exactly five times that in the lower crystal. The actual unit cell used in the simulation in this case is five times larger than this minimal unit cell, i.e., the length of the unit cell in the *x*-direction is $5(5 \times d_{101})$ or 6.366 nm.

All simulations were performed using MD, where the temperature is fixed using velocity rescaling and the crystal lattice parameters were chosen as appropriate for the simulation temperature. The interactions between the atoms are described using the Voter–Chen embedded atom method (EAM)[10] for nickel. The melting point was found to be 1626 ± 10 K for this interatomic potential as determined using the two-phase coexistence method.[11] This is approximately 100 K below the experimentally determined value (1728 K). This discrepancy is not critical for the present study, where the main focus is on the inclination dependence of grain boundary self-diffusion. Before any diffusivity or energy measurements were made, the initial simulation cell was heated to 1400 K and held for 0.6 ns; then the temperature was consequently dropped to the temperature of interest and held for an additional 0.6, 2.0, and 6 ns at $T = 1200$ K, 1000 K, and 900 K, respectively.

Self-diffusion coefficients were measured using the approach described by Schönfelder et al.[12] In this method, the grain boundary self-diffusion coefficient was determined from the slope of the in-plane mean-square displacement, $(\langle(\Delta x)^2\rangle + \langle(\Delta y)^2\rangle)$ versus time. While the boundary may roughen at high temperature, the mean boundary plane is always parallel to the *x-y* plane. This approach is therefore unaffected by boundary roughening or fluctuation in the mean boundary position (in the *z* directions). The grain boundary self-diffusivity is as follows

$$\delta D_{GB} = \frac{\sum_{i=1}^{N_{GB}} (\Delta x_i)^2 + (\Delta y_i)^2}{A} \frac{\Omega}{4t} \quad , \tag{1}$$

where A, δ, N_{GB}, and Ω are boundary area, grain boundary width, number of atoms in the grain boundary, and atomic volume, respectively. Clearly, the definitions of δ and N_{GB} are interrelated as

$$N_{GB} = A\delta/\Omega \quad , \tag{2}$$

and are both arbitrary. If the sum includes a sufficient number of atoms on either side of the boundary, the value of δD_{GB} is independent of δ and N_{GB} (typically we used $\delta = 3$ nm). Note that while δD_{GB} is well-defined, the grain boundary diffusivity D_{GB} itself, is not. δD_{GB} was determined by averaging over the atomic displacements for a sufficient time that the desired accuracy was obtained. In practice, this required simulations as long as 6 ns at the lowest temperature reported.

To understand the variation of grain boundary properties with boundary inclination, it would be useful to determine the grain boundary free energy as a function of the same geometrical parameter. While determining the grain boundary free energy is straightforward in simple systems,[13,14] accurate determination of the free energy versus temperature and inclination in systems with realistic interatomic potentials is much more complicated and requires substantial computational investments. On the other hand, the internal energy of the grain boundary may be determined much more efficiently. Therefore, we limit our investigation of the grain boundary thermodynamics to the measurement of grain boundary energy. To this end, we focus on a wide region of the simulation cell that includes the entire grain boundary and substantial

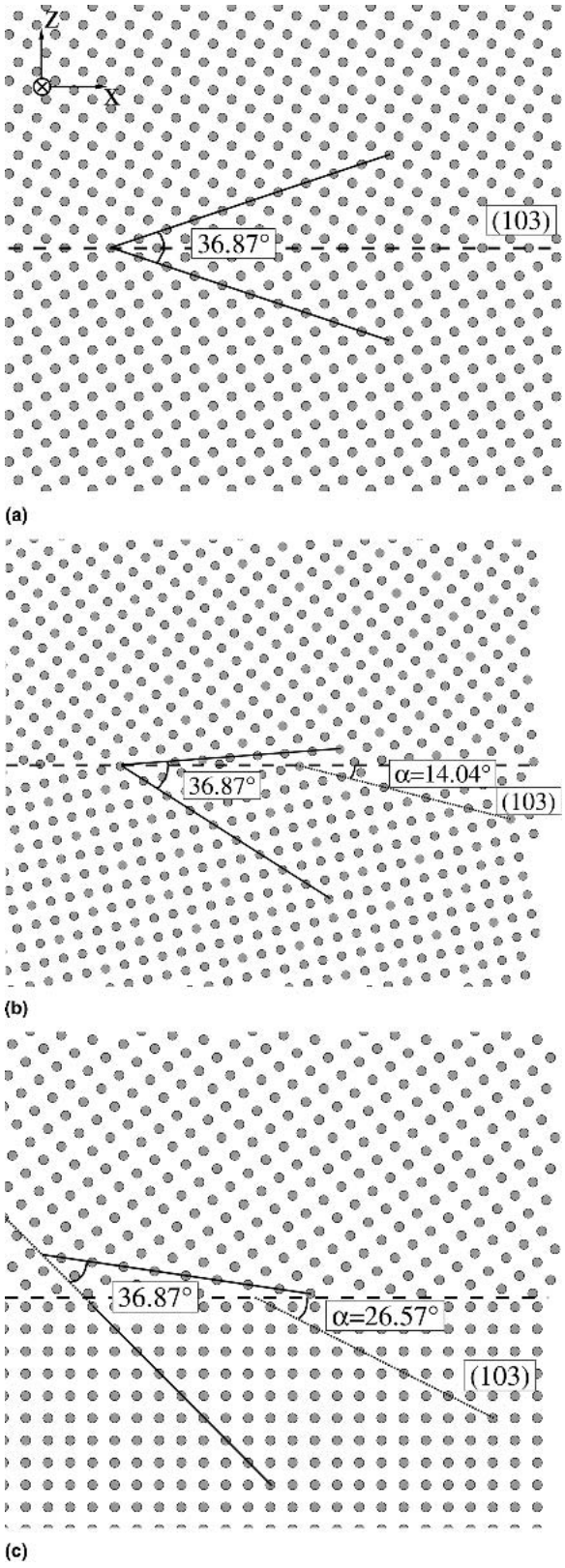

FIG. 1. Unrelaxed simulation cell for three different boundary inclinations of a $\Sigma 5$ [010] 36.87° tilt boundary: (a) $\alpha = 0°$, (b) $\alpha = 14.04°$, and (c) $\alpha = 26.57°$. The solid lines indicate {100} planes in the two crystals, the dashed line indicates the position of the boundary plane, and the dotted line indicates a (103) plane (used to define α).

regions of the bulk, but not those regions close to the two free surfaces. The internal energy E_i of all the atoms N in this region is averaged over a long simulation time. Since the total stress along the z direction and the stress in the bulk far away from boundary are zero (free surfaces in the z direction and periodic boundary conditions in x and y such that the appropriate temperature–dependent bulk lattice parameter is maintained), the grain boundary energy can be determined from the following expression

$$E_{\mathrm{GB}} = \left(\sum_{i=1}^{N} E_i - N E_{\mathrm{coh}} \right) / A \quad , \tag{3}$$

where E_{coh} is the cohesive energy per atom in the perfect crystal at the temperature of interest and A is the area of the cross section of the simulation cell parallel to the mean grain boundary plane.

III. TEMPERATURE DEPENDENCE OF GRAIN BOUNDARY STRUCTURE

The structure of a grain boundary can be very different at low and high temperature. Most experimental and computer simulation determinations of grain boundary structure were performed at temperatures much smaller than the melting point. Figure 2 shows the structure of the $\Sigma 5$ [010] symmetric tilt grain boundary (103) plane in Ni at $T = 0$ K, 1200 K, and 1400 K. The classical polyhedral structure of this boundary is indicated at $T = 0$ in Fig. 2(a). It is composed of a repeated pattern of kitelike arrangements of the atoms at the boundary plane. When this structure is heated to and held at 1200 K [Fig. 2(b)], the same kitelike structure is preserved. However, at this elevated structure the kites are highly distorted. When the temperature is raised further [to 1400 K; Fig. 2(c)], it is no longer possible to resolve the underlying kitelike structure except in a small number of isolated locations in the boundary plane. Further, at this temperature, the boundary does not remain planar. Given the change in boundary structure seen upon heat the system, we should expect the grain boundary properties to vary strongly with temperature. Further, discussion of the grain boundary diffusivity in terms of the ideal low temperature structure will be speculative at best.

Another important distinction between grain boundaries at high and low temperature is the boundary mobility. In Fig. 3, we show the mean position of the boundary in the z-direction (i.e., averaged over the boundary plane; see Fig. 1) versus simulation time at 900 K, 1200 K, and 1400 K. Even with no external driving force, the boundary can wander a significant distance at high temperature. The mean squared displacement at 1400 K is 100 times larger than that at 900 K. Since the boundary wanders so quickly compared to most experimental

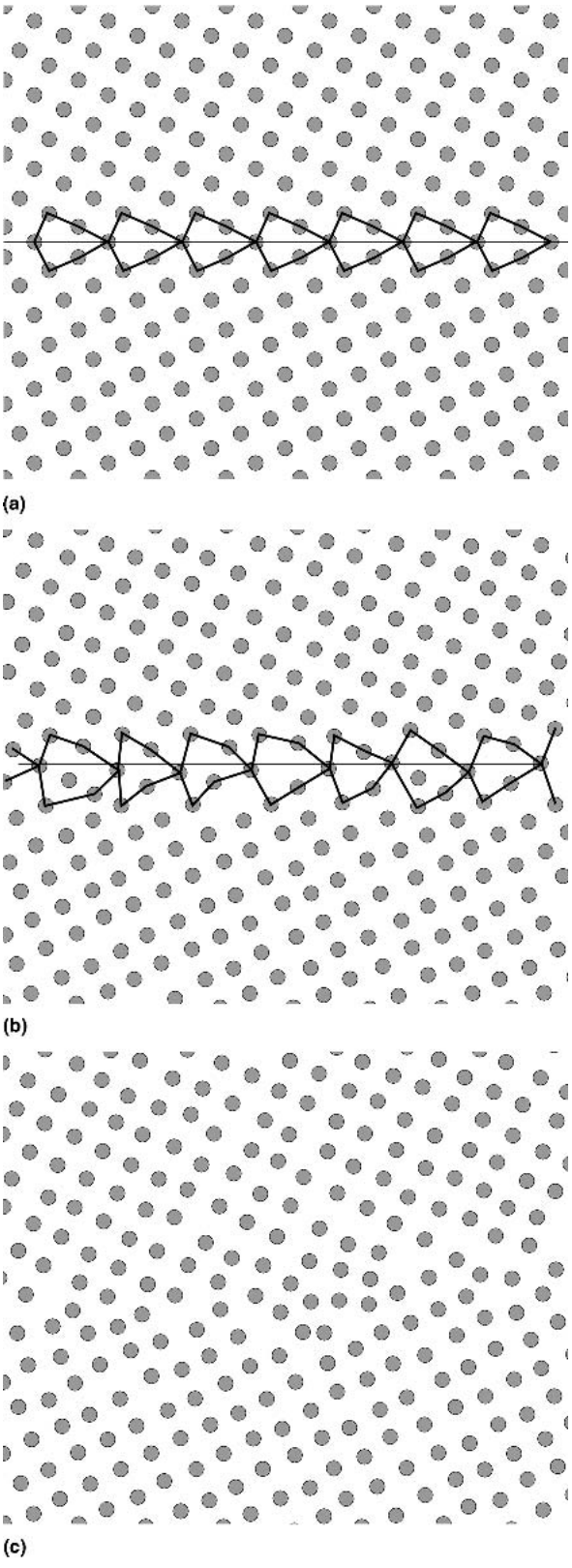

FIG. 2. $\alpha = 0°$ symmetric grain boundary at different temperatures, (a) $T = 0$ K, (b) $T = 1200$ K, and (c) $T = 1400$ K. Plausible structural units are indicated at the lower temperature. The disorder in the boundary makes such a structural unit description of limited use at the highest temperature.

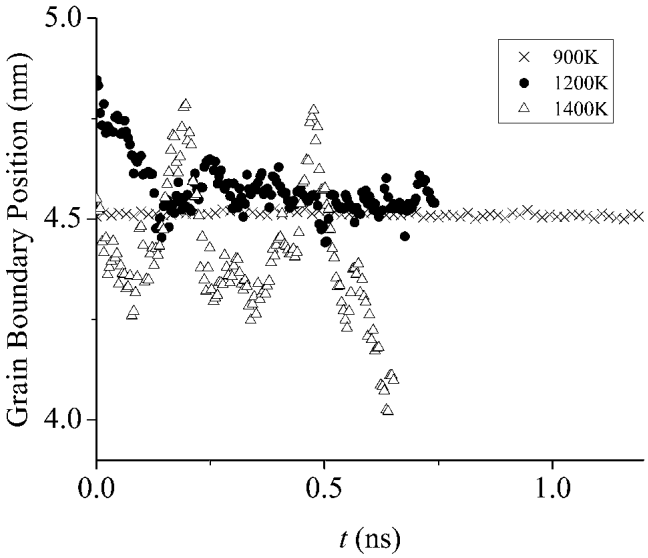

FIG. 3. The mean position of the $\alpha = 0°$ grain boundary versus simulation time at different temperatures.

measurement of grain boundary properties, the structure of the boundary at high temperature is inherently a time average over the boundary's wanderings. This is potentially very important for grain-boundary diffusion as a wandering boundary could potentially leave the labeled diffusant behind and may reacquire it later. The importance of such an effect will depend on the mobility of the diffusant and the degree of binding of the diffusant to the boundary. This suggests that high-temperature and low-temperature grain-boundary diffusion could be quite different.

IV. GRAIN BOUNDARY SELF-DIFFUSION

A typical mean-square displacement $\langle R^2 \rangle$ for Ni atoms initially in a Ni (103) symmetric tilt grain boundary is shown in Fig. 4 as a function of time at three different temperatures. The mean-square displacement is a linear function of time at all temperatures examined. The slope of these lines, according to Eq. (1), is the product of the boundary width and self-diffusion coefficient δD. Figure 4 shows that δD is a strong function of temperature, increasing by two orders of magnitude when the temperature is raised from 900 K to 1400 K. Because of this, long simulations are required to determine δD at low temperature.

Figure 5 shows δD as a function of grain boundary inclination at 900–1400 K. These data show that δD is much more anisotropic at low temperature than at high temperature. At 1400 K, δD varies from 3.1×10^{-13} to 3.5×10^{-13} cm^3/s, while at 900 K it varies from 2.6×10^{-15} to 3.7×10^{-14} cm^3/s as the inclination is varied. The diffusivity shows a maximum at $\alpha = 21.8°$, a minimum at $\alpha = 26.6°$, and another maximum at $\alpha = 31.0°$

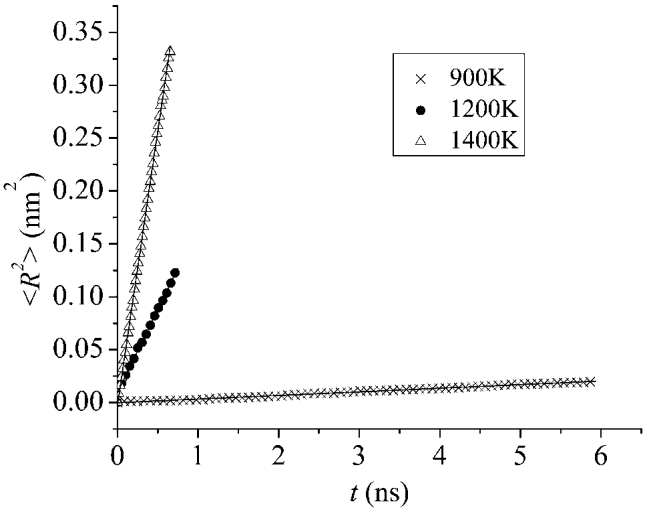

FIG. 4. Mean-square displacement of the atoms in the $\alpha = 0°$ grain boundary versus simulation time at three different temperatures.

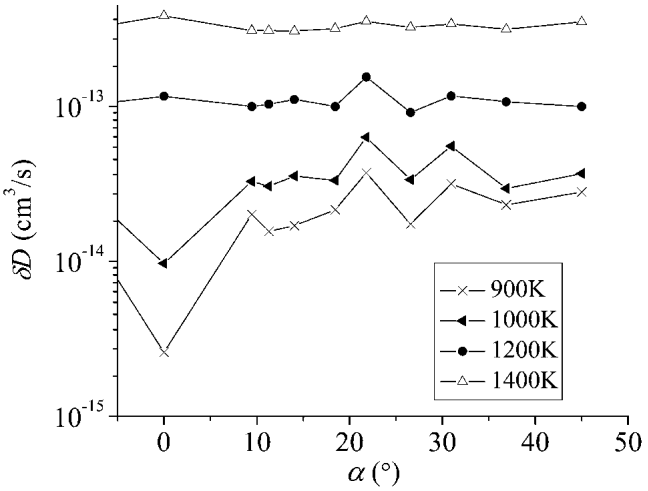

FIG. 5. Logarithm of the grain boundary self-diffusion coefficient δD as a function of grain boundary inclination at different temperatures.

at all temperatures. Interestingly, the minimum in the diffusivity at $\alpha = 26.6°$ corresponds to an inclination for which the grain boundary plane is a low index plane in one of the two grains, i.e., (110). At low temperature (below 1200 K), the global minimum in the grain boundary diffusivity δD occurs at $\alpha = 0°$. At high temperaturez (1200 K and above), the grain boundary diffusivity is a maximum. The $\alpha = 0°$ grain boundary is symmetric and is also special in the sense that boundary plane is a high density plane in both grains; i.e., the (103) plane.

The change in δD for $\alpha = 0°$ from being a minimum with respect to inclination to a maximum suggests that the activation energy for diffusion for this boundary is larger than that of the boundaries with nearby inclinations. We examine this statement more qualitatively by plotting δD versus T in Arrhenius coordinates in Fig. 6 for each inclination. Within the accuracy of the simulations,

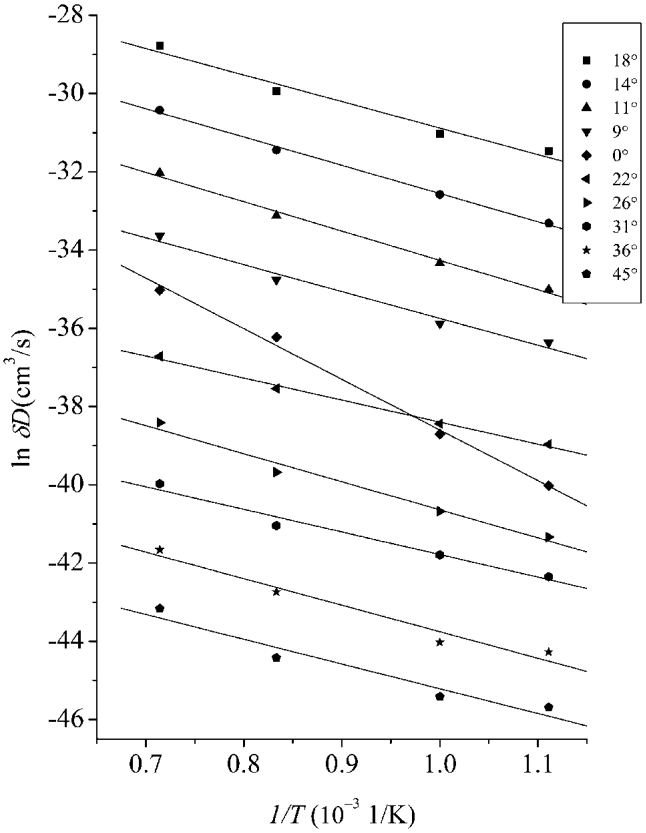

FIG. 6. Logarithm of the grain boundary self-diffusion coefficient δD versus the inverse temperature for ten different boundary inclinations. For clarity, all of the curves have been arbitrarily shifted with respect to each other.

the data all fall on the same straight line for each inclination. The slope of these lines is $-Q/k_B$, where Q is the activation energy for grain boundary self-diffusion. The slopes (activation energies) for all inclinations appear to fall within a very narrow band, except for the $\alpha = 0°$ case. For this case, the activation energy is larger than for all other inclinations, as suggested above. Figure 7 explicitly shows the activation energies for grain boundary self-diffusion as a function of inclination. Indeed, the activation energy all lie between 0.5 to 0.6 eV, except for the symmetric boundary ($\alpha = 0°$), which is 1.1 eV.

Although the activation energy for boundary self-diffusion varies with inclination (by as much as a factor of two), the actual variation in the boundary self-diffusion coefficient can be significantly smaller (e.g., see Fig. 5 at 1400 K). This is because the boundary self-diffusion coefficient is Arrhenius $\delta D = \delta D_0 e^{-Q/k_B T}$, where the pre-exponential factor δD_0 may also vary with boundary inclination. Figure 8 shows the logarithm of the pre-exponential factor δD_0 versus the activation energy for self-diffusion Q for all of the simulation data presented above. This data clearly shows that these two quantities are proportional to one another. Therefore,

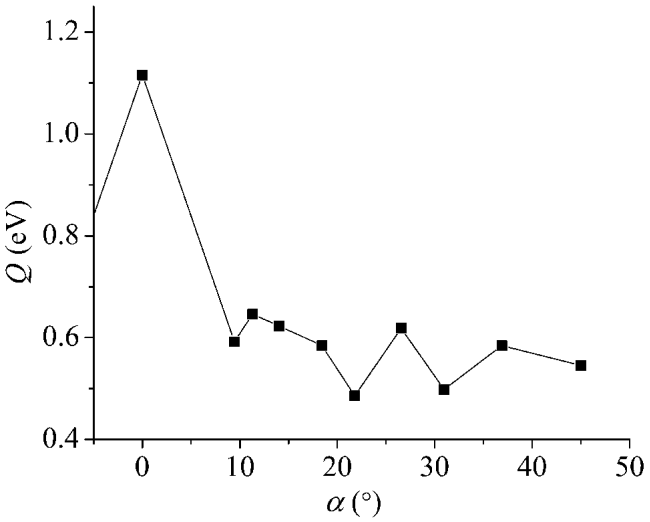

FIG. 7. Activation energy for grain boundary self-diffusion versus grain boundary inclination.

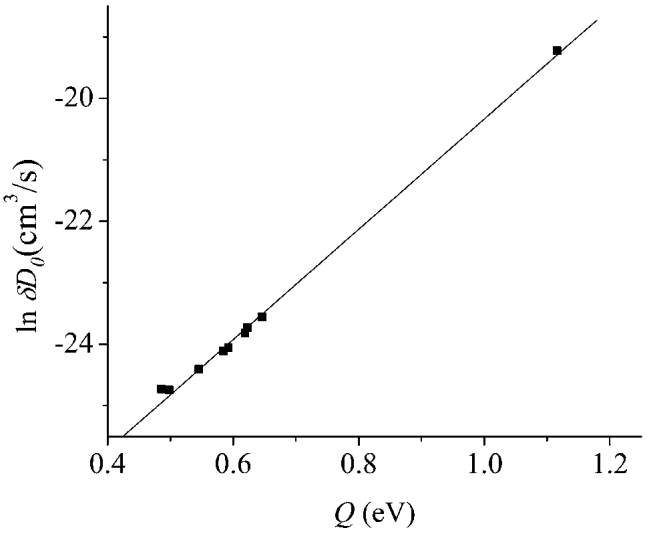

FIG. 8. Natural logarithm of the pre-exponential factor versus activation energy for grain boundary self-diffusion.

increases in the activation energy with α are largely compensated by similar increases in $\ln(\delta D_0)$. This has the effect of diminishing the effect of variations in the activation energy with boundary inclination. This compensation effect phenomenon has been reported earlier in other systems.[15,16]

V. DISCUSSION AND CONCLUSION

In this paper, we examined grain boundary self-diffusion in Ni using molecular dynamics simulations. Our main focus was the effect of boundary inclination on the grain boundary self-diffusion coefficient in a series of Σ5 [010] tilt boundaries. The boundary self-diffusion coefficient was observed to vary strongly with boundary inclination at low temperature and only weakly at high temperature. At 900 K, the ratio between the maximum and minimum diffusivity is larger than 10, while at 1400 K it is reduced to 1.3. Therefore, we expect the self-diffusivity to be nearly inclination independent close to the melting temperature. This implies that the boundary self-diffusion coefficient is sensitive to the detailed atomic structure of the boundary at low temperature but not at high temperature.

The nature of the variation of the boundary self-diffusion coefficient with inclination can be understood by examining some gross crystallographic feature of the grain boundary. In particular, the minima in the grain boundary diffusivity with respect to inclination correspond to boundaries for which the boundary plane is a low index plane in at least one of the two crystals. For example, the minimum at $\alpha = 0°$ is for a boundary plane that is a (103) plane in both crystals; that at 26.6° is a (101) plane in one of the crystals; and that at 36.9° is a (103) plane in one of the crystals. However, not all low index boundary planes correspond to minima in the diffusivity [e.g., $\alpha = 45°$ corresponds to (102) planes of both crystals]. Interestingly, the boundary diffusivity switches from a minimum to a maximum with increasing temperature in the $\alpha = 0°$ case. It does, nonetheless, continue to be an extremum of the diffusivity at all temperatures examined.

More insight into the effect of inclination on grain boundary diffusivity can be gained by examining the boundary energy as a function of the same inclination. Figure 9 shows the grain boundary energy (not free energy) as a function of inclination. Interestingly, the $\alpha = 0°$ boundary has minimum energy at 900 K and 1000 K and is a maximum at 1200 K and 1400 K, in agreement with the variation seen in the grain boundary diffusivity. Similarly, the minima in the diffusivity at $\alpha = 26.6°$ and

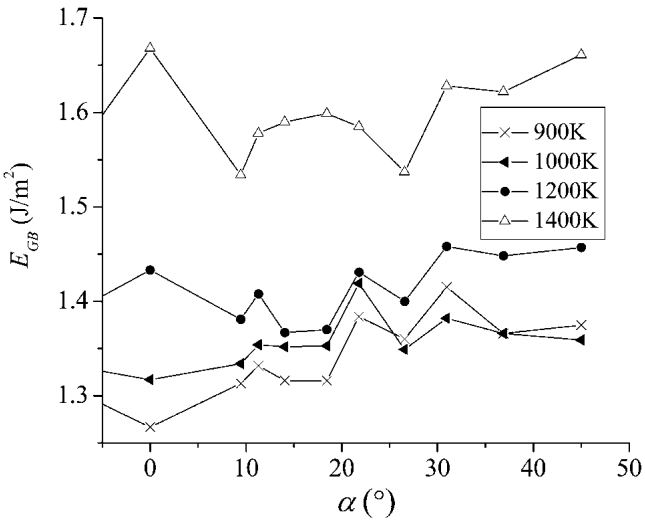

FIG. 9. Grain boundary energy as a function of grain boundary inclination at different temperatures.

36.9° also correspond to minima in the grain boundary energy with respect to inclination (the trend is not very clear at $\alpha = 36.9°$, though). A more careful examination of the grain boundary energy versus inclination behavior shows very good agreement with the behavior seen in the boundary diffusivity versus inclination (Fig. 5). In particular, there is generally good agreement between positions of the minima and maxima in these two plots at all temperatures.

We found that the self-diffusion coefficients may be reasonably described using an Arrhenius relation. However, careful examination of Fig. 6 shows that the 900 K and 1400 K data routinely lie slightly above the best fit Arrhenius line. On the other hand, omitting the 1400 K data would allow a single Arrhenius line to be drawn through the lower temperature data. This is not surprising since, as shown in Fig. 2, the structure of the boundaries at 1400 K appears to be significantly more disordered than those at 1200 K or less. Therefore, a change in diffusion mechanism between 1200 K and 1400 K may be responsible for the small deviation of the data from an Arrhenius line in Fig. 6.

It is reasonable to assume that there is a correlation between the density of and the activation energy for diffusion in grain boundaries in close packed materials. In the present case, we note that, by far, the largest activation energy for diffusion occurs at the $\alpha = 0°$ boundary (see Fig. 7). At this inclination, the boundary plane corresponds to (103) planes in both crystals (i.e., it is a symmetric tilt boundary). This is (by far) the highest density boundary in the series considered in this study. Examination of Fig. 7, shows that the activation energies for diffusion in the other boundaries all vary within a relatively small range. If we characterize the density of the boundary as the inverse of the boundary unit cell size ($T = 0$), we find that the local minima in the activation energies for diffusion that occur at 9.5°, 21.8°, and 31.0° (see Fig. 7) correspond to local minima in the boundary density. In addition, the $\alpha = 26.6°$ boundary is a local maximum in both the activation energy for boundary diffusion and the density and corresponds to a structure with a (101) boundary plane (in one of the two crystals). We also performed a series of simulations for [001] 36.87° twist boundaries using the same interatomic potential. In this case, the grain boundary is also very dense. The activation energy for boundary diffusion in this case was found to be 1.09 eV. This is very close to the activation energy for the highest density tilt boundary ($\alpha = 0°$) we reported above, i.e., 1.1 eV. Taken together, these data suggest that relatively high boundary plane densities correspond to relatively high activation energies for self-diffusion. Note that these activation energies are somewhat lower than those found in experiments (1.0–1.9 eV).[4–9] This discrepancy is not surprising given that the experimental data are averaged over the misorientation and inclination distribution of a polycrystals (or a general tilt boundary) and the present simulations were performed using only the very special $\Sigma 5$ misorientation.

The compensation effect (i.e., the proportionality between the activation energy and the logarithm of the pre-exponential factor in the Arrhenius relation) has been observed in a wide range of physical situations where the events are thermally activated,[15] including many cases of interfacial diffusion.[16] There are no reports in the literature (to our knowledge) that present the existence of a compensation effect for grain-boundary diffusion as a function of boundary inclination (perhaps due to the paucity of experimental or simulation data). Since the present results demonstrate that the activation energy for grain-boundary diffusion is proportional to the logarithm of the pre-exponential factor in the Arrhenius form of the diffusivity (Fig. 8), variations in the diffusivity with inclination are much weaker than would be expected on the basis of the behavior of the activation energy with inclination (Fig. 7). For example, at $T = 900$ K, the difference in activation energy between $\alpha = 0°$ and $\alpha = 26.6°$ suggest a difference in the grain boundary self-diffusion coefficient of ~3000, while the data in Fig. 5 shows that this variation is more than two orders of magnitude smaller (a factor of ~14). Therefore, extreme caution must be exercised in trying to estimate how diffusivities vary solely on the basis of activation energies (as is commonly done).

ACKNOWLEDGMENTS

The authors gratefully acknowledge the support of the United States Department of Energy, Grant No. DE-FG02-99ER45797 and the Computational Materials Science Network.

REFERENCES

1. V.Y. Aristov, V.L. Mirochnik, and L.S. Shvindlerman: Mobility of (111) intergrain tilt boundary in aluminum. *Sov. Phys. Solid State* **18,** 137 (1976).
2. M. Upmanyu, D.J. Srolovitz, L.S. Shvindlerman, and G. Gottstein: Misorientation dependence of intrinsic grain boundary mobility: Simulation and experiment. *Acta Mater.* **47,** 3901 (1999).
3. D. Wolf: Correlation between energy and volume expansion for grain-boundaries in fcc metals. *Scripta Metall. Mater.* **23,** 1913 (1989).
4. W.R. Upthegrove and M.J. Sinnott: Grain boundary self-diffusion of nickel. *Trans. ASM* **50,** 1031 (1958).
5. A.R. Wazzan: Lattice and grain boundary self-diffusion in nickel. *J. Appl. Phys.* **36,** 3596 (1965).
6. W. Lange, A. Hassner, and G. Mischer: Measurement of grain-boundary diffusion of Ni^{63} in Ni and γ-Fe. *Phys. Status Solidi* **5,** 63 (1964).

7. M. Jurisch and A. Hassner: Concentration depletions and enhancements in range of grain boundaries. *T. Jpn. I Met.* **10,** 439 (1969).
8. R.F. Canon and J.P. Stark: Grain boundary self-diffusion in nickel. *J. Appl. Phys.* **40,** 4366 (1969).
9. N.W. Dereca and C.A. Pampillo: Grain-boundary diffusivity via bulk diffusion measurements during grain-growth. *Scripta Metall. Mater.* **9,** 1355 (1975).
10. A.F. Voter and S.P. Chen: Accurate interatomic potentials for Ni, Al and Ni_3Al, in *Characterization of Defects in Materials,* edited by R.W. Siegel, J.R. Weertman, and R. Sinclair (Mater. Res. Soc. Symp. Proc. **82,** Pittsburgh, PA, 1987), p. 175.
11. J.R. Morris, C.Z. Wang, K.M. Ho, and C.T. Chan: Melting line of aluminum from simulations of coexisting phases. *Phys. Rev. B* **49,** 3109 (1994).
12. B. Schönfelder, D. Wolf, S.R. Phillpot, and M. Furtkamp: Molecular-dynamics method for the simulation of grain-boundary migration. *Interface Sci.* **5,** 245 (1997).
13. M.T. Lusk and P.D. Beale: Grain-boundary free energy in an assembly of elastic disks. *Phys. Rev. E* **69,** 026117 (2004).
14. B.L. Adams, D. Kinderlehrer, W.W. Mullins, A.D. Rollett, and S. Ta'asan: Extracting the relative grain boundary free energy and mobility functions from the geometry of microstructures. *Scripta Mater.* **38,** 531 (1998).
15. W. Meyer and Z. Neldel: Relationship between the energy constant ϵ and the mass constant α in the conductivity-temperature formula for oxydic semiconductors. *Z. Tech. Phys.* **12,** 588 (1937).
16. G. Boisvert, L.J. Lewis, and A. Yelon: Many-body nature of the Meyer–Neldel compensation law for diffusion. *Phys. Rev. Lett.* **75,** 469 (1995).